
AN INTERCONNECTED SYSTEM OF ENERGY

A PREPRINT

Husam Wadi
hwadi@andrew.cmu.edu *

ABSTRACT

In this paper, I aim to describe a system of interconnected energy models. These models produce inferences that may enhance our understanding of classical and quantum mechanics. From the formulated models, an empirical test is derived to validate the proposed light projection hypothesis.

1 Introduction

It is understood that a chasm exists between our classical understanding of relativity [7] and the subatomic descriptions of quantum mechanics [4]. Many theories provide solutions to this discrepancy: from superstrings [21] to loop quantum gravity [24] and other numerous paradigms, each with their significant contributions to furthering our knowledge of theoretical physics. The system of models I present provides a foundation for reframing the underlying assumptions of special relativity [10] and an alternate description of quantum activity [23]. By simplifying our understanding of time, we are able to shift to homogeneous coordinates as a viable basis. From homogeneous coordinates, we can create a spatial framework of reality. The spatial framework allows us to hypothesize the function of black holes and discern the projections of higher dimensions of light. The projections of light hint toward a cosmic camera obscura that a pinhole camera matrix can model. We can then view the entire structure through a different lens and relate the layers of light projections to a Deep Restricted Boltzmann Network (DRBN) [16] representation of quantum information.

2 Time-energy equivalence

The first matter to establish is the relationship between time and energy. Time is necessary for defining the speed of light, on which matter-energy equivalence [9] and special relativity depend. However, it would not be precise to determine time by the absolute motion of light as that definition crumbles when a reference particle's motion (energy) interferes with the movement of a photon (energy transfer) towards another particle of vibrating matter (also energy). If we fire a photon from a fixed frame, the frame is neither fixed nor inertial if it is the collection of sporadically accelerating subatomic wave-particles.

In light of this, these are the definitions I will utilize:

1. **Energy:** The ability to change states, namely motion.
2. **Time:** The measurement of energy interactions, the difference of motion.
3. **Dimension:** The number of coordinates required to specify motion.
4. **Time-Energy Equivalence:** If the measurement of energy transfer (difference of motion) and matter (motion) cannot be distinctly separated, then they will be treated as equivalent properties.

Time-energy equivalence is defined by Eq. (1). A change in time is equal to a change in energy. With this equation in place, it is possible to convert between a unit of time, such as a second, and a unit of energy as shown in Eq. (2)

$$\Delta t = \Delta E \tag{1}$$

*For more information please visit <https://hwadi.io>

$$1s = 1e_u \quad (2)$$

Evidence for time-energy equivalence can be found in the use of the Compton wavelength [13] derived from the mass of a particle as an oscillatory frequency in which a reference clock can be developed. A mass-based Compton clock has been produced and tested by Shau-Yu Lan et al. in 2013 [18].

3 Homogeneous spacetime representation

With time and energy as equivalent properties, we can simplify the notion of *spacetime and matter* to *space and energy*, denoted as *dimensional-energy*. Dimensional-energy, with coordinates $u, v, & w$ resides in a Euclidean space, and spacetime-matter, with coordinates $x, y, z, & t$ resides in a homogeneous space. Eq. (3) describes the relation between the two spaces.

$$\begin{bmatrix} u \\ v \\ w \end{bmatrix} = \begin{bmatrix} u \\ v \\ w \\ 1 \end{bmatrix} = \begin{bmatrix} x/t \\ y/t \\ z/t \\ 1 \end{bmatrix} = \begin{bmatrix} x \\ y \\ z \\ t \end{bmatrix} \quad (3)$$

Time is the additional $n+1$ -dimensional homogeneous scale factor, that when divided by, results in a n -dimensional Euclidean velocity space. These spacetime velocities are **equivalent** to dimensional-energy spatial coordinates. From the opposite perspective, spatial dimensions in spacetime equal the absence of dimensional-energy. Both relations are shown in Eq. (4).

$$\begin{aligned} u &= x/t, & x &= u \cdot t \\ v &= y/t, & y &= v \cdot t \\ w &= z/t, & z &= w \cdot t \end{aligned} \quad (4)$$

For clarity, these are the definitions I will use in dimensional descriptions:

1. A number followed by the letter D denotes spatial coordinates only. For example, A $4D$ space denotes a location where four-dimensional shapes are possible.
2. A spatial dimension followed by $+1$ denotes the addition of a perceived projective time component. Our observable universe is $3D+1$ as we have three spatial dimensions plus one of time. A $4D+1$ layer represents a location where four-dimensional shapes and time are reality.

By employing the decades of research in superstring theory as a basis, we can create a model of reality that is ten-dimensional to agree with Type I, IIA, IIB, HO, & HE superstring theories [26]. This $10D$ space cascades through layers of projections down to a $3D$ space. The $10D$ Euclidean input layer is denoted with $x, y, z, & t$ for the dimensions we are familiar with and $a, b, c, d, f, & e$ for the extra six dimensions we are unfamiliar with. The last term is kept as e to represent the full span of $10D$ energy. To shift from $10D$ to $9D+1$ we divide by the last term, e , and then drop the underlying 1 to convert into a $9D$ Euclidean space as demonstrated in Eq. (5).

$$\begin{bmatrix} x \\ y \\ z \\ t \\ a \\ b \\ c \\ d \\ f \\ e \end{bmatrix} \rightarrow \begin{bmatrix} x/e \\ y/e \\ z/e \\ t/e \\ a/e \\ b/e \\ c/e \\ d/e \\ f/e \\ 1 \end{bmatrix} \rightarrow \begin{bmatrix} x/e \\ y/e \\ z/e \\ t/e \\ a/e \\ b/e \\ c/e \\ d/e \\ f/e \end{bmatrix} \quad (5)$$

We can then shift from a $9D$ Euclidean space to a $8D$ Euclidean space by dividing by the scale factor, f/e , as shown in Eq. (6).

$$\begin{bmatrix} x/e \\ y/e \\ z/e \\ t/e \\ a/e \\ b/e \\ c/e \\ d/e \\ f/e \end{bmatrix} \rightarrow \begin{bmatrix} \frac{x/e}{f/e} \\ \frac{y/e}{f/e} \\ \frac{z/e}{f/e} \\ \frac{t/e}{f/e} \\ \frac{a/e}{f/e} \\ \frac{b/e}{f/e} \\ \frac{c/e}{f/e} \\ \frac{d/e}{f/e} \\ 1 \end{bmatrix} \rightarrow \begin{bmatrix} x/f \\ y/f \\ z/f \\ t/f \\ a/f \\ b/f \\ c/f \\ d/f \end{bmatrix} \quad (6)$$

The e term cancels out from f/e and we are left with the variables in the $8D$ Euclidean space divided by f . We can reason about why this happens geometrically if we visualize a $3D$ object being projected into a $1D$ space as shown in Fig. 1.

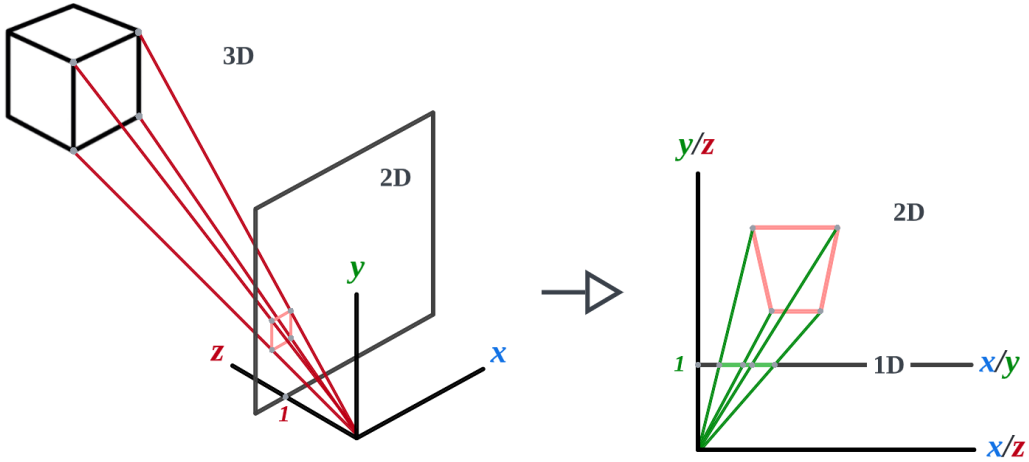


Fig. 1: 3D to 1D projection

Once the projection collapses into a single dimension, the z -axis from the $3D$ space is no longer relevant. However, it played a significant role in forming the $2D$ projection shape, resulting in the location and size of the $1D$ silhouette. Eq. (7) demonstrates the completed projection model from $10D$ to $3D$.

$$\begin{bmatrix} x \\ y \\ z \\ t \\ a \\ b \\ c \\ d \\ f \\ e \end{bmatrix} \rightarrow \begin{bmatrix} x/e \\ y/e \\ z/e \\ t/e \\ a/e \\ b/e \\ c/e \\ d/e \\ f/e \end{bmatrix} \rightarrow \begin{bmatrix} x/f \\ y/f \\ z/f \\ t/f \\ a/f \\ b/f \\ c/f \\ d/f \end{bmatrix} \rightarrow \begin{bmatrix} x/d \\ y/d \\ z/d \\ t/d \\ a/d \\ b/d \\ c/d \end{bmatrix} \rightarrow \begin{bmatrix} x/c \\ y/c \\ z/c \\ t/c \\ a/c \\ b/c \end{bmatrix} \rightarrow \begin{bmatrix} x/b \\ y/b \\ z/b \\ t/b \\ a/b \end{bmatrix} \rightarrow \begin{bmatrix} x/a \\ y/a \\ z/a \\ t/a \end{bmatrix} \rightarrow \begin{bmatrix} x/t \\ y/t \\ z/t \end{bmatrix} \quad (7)$$

In Fig. 2 a spatial model of dimensional-energy is formulated from Eq. (7). Each layer is labeled with an integer, the number of independent dimensions plus homogeneous time factor if applicable, and the projected time/energy variable that will be utilized extensively in Sec. 5.

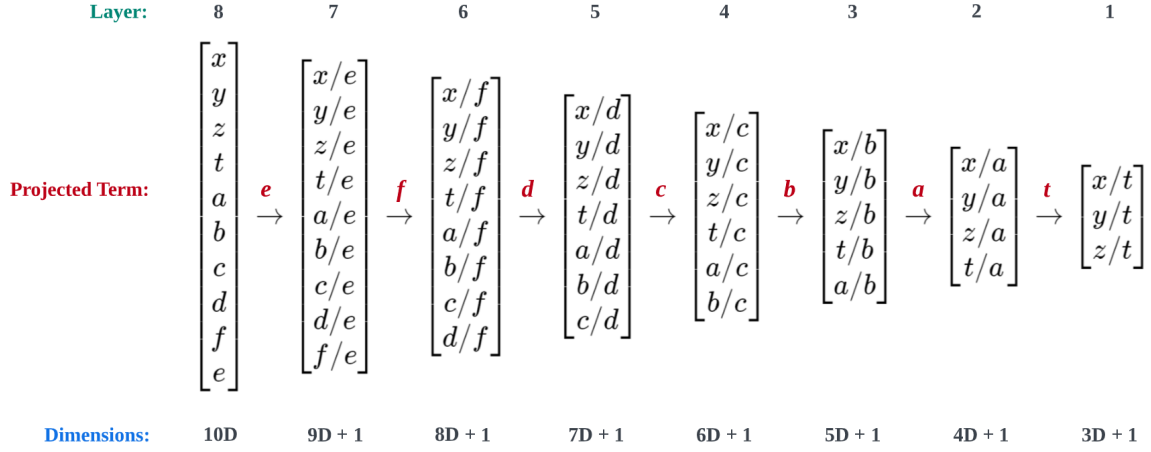


Fig. 2: Spatial model of dimensional-energy in spacetime coordinates

Notice that we are labeling these dimensions as $ND+1$ since we are using spacetime variables. A true dimensional-energy representation would require a separate variable for each term, as x/e **does not** equal x/f , or x/d , or x/c , etc.

If we focus on the spatial dimensions of the model, a point inserted into $3D$ space would appear as a line of possibilities in $4D$ space. A point is zero-dimensional as it has no attributes such as length, width, or height. A $0D$ point in $3D$ space expands into a $7D$ hypercube of possibilities in a $10D$ space. These representations could be modeled as manifolds, with the highest dimension being $7D$.

A physical attribute that manifests from this model is the difference between the $9D+1$ and the $10D$ layer. There is no longer a projection factor in the $10D$ layer, and time, in any meaningful manner, ceases to exist. Another physical attribute is that time, t , itself in the $3D+1$ layer results from the collapsed higher-layer projections e , f , d , c , b , & a .

Localizing a point in $4D$ space from a $3D$ space requires reconstructing that point with more than one reference frame. Epipolar geometry can be utilized to define $3D$ point triangulation using uncalibrated $2D$ camera planes. This epipolar technique can be extended to define higher-dimensional points within a $3D$ space, which has been explored by Saba Miyan and Jun Sato. [20]. Another technique called *4D tensor voting*, by Wai-Shun Tong et al. [30], estimates epipolar geometry by applying local geometric smoothness constraints in $4D$ joint image space. There may be a causal connection between this higher-dimensional perspective-dependent property and quantum indeterminacy as explored by Chris Fields et al. [12]. Other aspects of cosmology, such as curvature singularities, conformal infinity, and matter flow lines, also appear as properties of projective geometric spaces as shown in Thomas Hurd's formulations [17].

4 Black holes & light projections

The universe modeled as existing inside a higher-dimensional black hole is by no means a novel concept. Prior literature of this postulation includes theorizations by Razieh Pourhasan et al. [22] & Jose B. Almeida [3]. I will extend this idea to include a black hole for every layer in the spatial model: the black hole acts as a dimension-reducing agent that projects the layer above it. This black hole projection can be viewed as conceptually related to Leonard Susskind's derivation of the holographic principle [29].

From the homogeneous projections, I hypothesize that the speed of light in each layer depends on the speed of light and the radius of the encapsulating black hole in the layer preceding it as shown in Tab. 1. Since the $10D$ layer exists outside of any time projection, I posit that it cannot be measured directly in any meaningful manner and set its light speed to infinity. However, all other sublayers are projections like our layer, can be measured, and are reachable by our faculties and instruments.

Tab. 1: Functions of the speeds of light

Dimensions	Speed of Light
$10D$	∞
$9D+1$	$c_9 = f(c_{10}, r_{10})$
$8D+1$	$c_8 = f(c_9, r_9)$
$7D+1$	$c_7 = f(c_8, r_8)$
$6D+1$	$c_6 = f(c_7, r_7)$
$5D+1$	$c_5 = f(c_6, r_6)$
$4D+1$	$c_4 = f(c_5, r_5)$
$3D+1$	$c_3 = f(c_4, r_4)$

I will utilize wheel theory [6] as a model for black holes. The radius of the black hole will be defined as the radius r of the wheel. Since the black hole collapses a dimension from the higher $(N+1)D+1$ layer, there is **no real** interior inside the black hole. All that exists is the infinite edge which represents the $ND+1$ universe as shown in Fig. 3. The center of the wheel, the nullity point Ω , represents the singularity of the black hole.

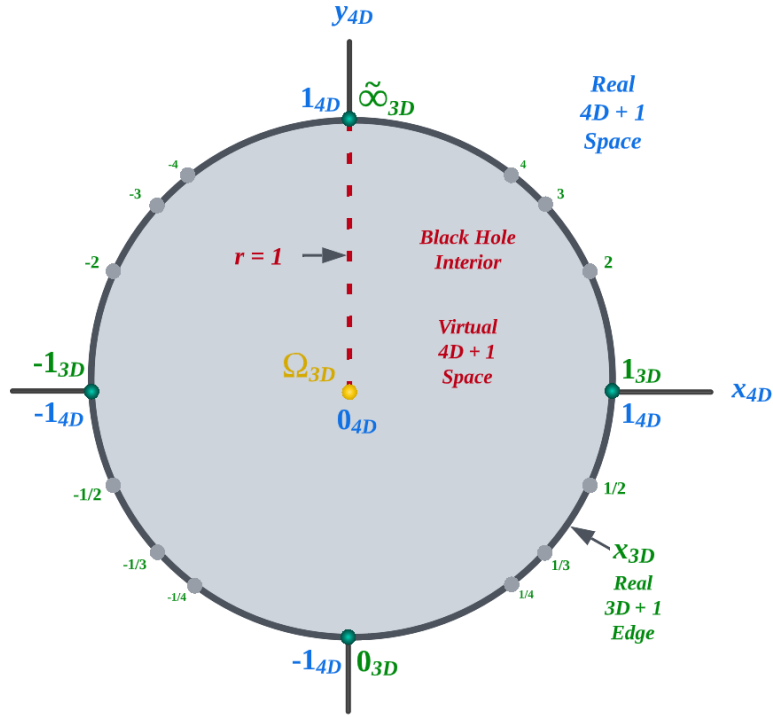


Fig. 3: 4D+1 to 3D+1 projective black hole

The manner in which we can reason about the interior of the black hole is similar to how we reason about virtual images in a convex mirror. It would appear as though a light ray has traveled into the black hole, but in reality, it interacts only on the surface, and its faint reflection creates the appearance of interior travel. From the work of Sreenath Manikandan and Andrew Jordan [19], there may be evidence supporting the interpretation of a black hole as a superconducting surface that facilitates Andreev reflections forming cooper pairs. This pairing property has also been recently explored for photons interacting with superconductors in a paper by André Saraiva et al. [25].

I will stipulate that any real $(N+1)D+1$ light touching the black hole's event horizon becomes a virtual $(N+1)D+1$ ray that is projected to the $ND+1$ complex infinity. Once at the infinite point, the virtual light ray is emitted from the black hole's singularity and projected on the real $ND+1$ surface as shown in Fig. 4.

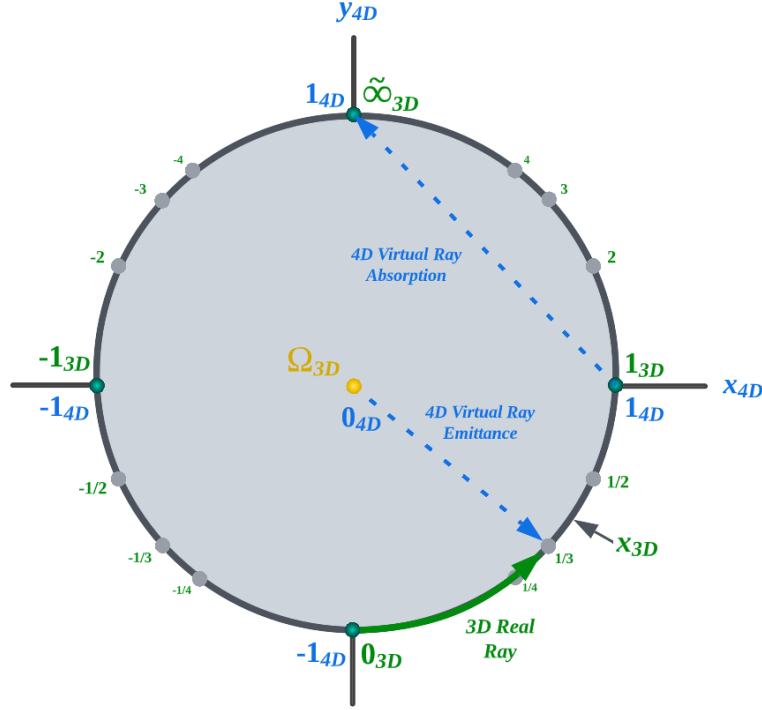


Fig. 4: 4D virtual light projection into 3D real light

This projection model will be combined with a $(N+1)D+1$ spacetime velocity diagram that conforms to special relativity. I hypothesize that the $(N+1)D+1$ speed of light can be regarded as constant with respect to the $ND+1$ layer beneath it. The y -axis will represent the velocity of time v_t and the x -axis will represent the velocity of space v_s . A real $(N+1)D+1$ photon moving through this diagram will give 100% of its velocity to space and 0% of its velocity to time as shown in Fig 5. To combine the diagrams, we center the axes on the $(N+1)D+1$ special relativity coordinate frame and place the black hole projection to the left of the origin. Exploring what happens when we try to project the virtual speed of $(N+1)D+1$ light into the black hole, we find several physical constraints on the $(N+1)D+1$ virtual photon as shown in Fig. 6. The physical constraints are:

1. We cannot project a $(N+1)D+1$ virtual photon to the $ND+1$ complex infinity without inducing a time component, and thus some form of virtual mass.
2. The point at infinity is unreachable without the ability to scale the virtual $(N+1)D+1$ speed of light.

To solve these constraints, we will allow the absorbed virtual photon to exceed the $(N+1)D+1$ light speed. However, for the emitted virtual ray, we divide the $(N+1)D+1$ light speed by the excess absorption speed to preserve special relativity globally as shown in Fig 7. The equation based on this formulation for the $3D+1$ to $4D+1$ speeds of light is described in Eq. (8).

$$c_3 = \left| \frac{-c_4}{r\sqrt{2}} \right| \quad (8)$$

$$c_3 = \frac{c_4}{r \cdot \sqrt{2}}$$

The negative sign in the numerator denotes that the virtual ray is pointing opposite to the original direction of the $(N+1)D+1$ light. In the lower $ND+1$ space, there may be no measurable way to tell that the speed is inverted, so the absolute value is what is effectively perceived.

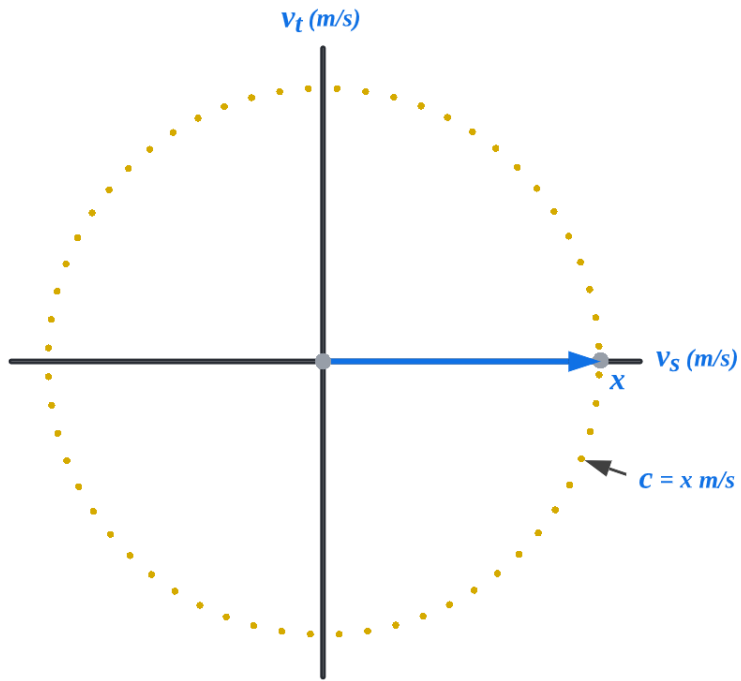


Fig. 5: A (N+1)D+1 photon with special relativity constraint

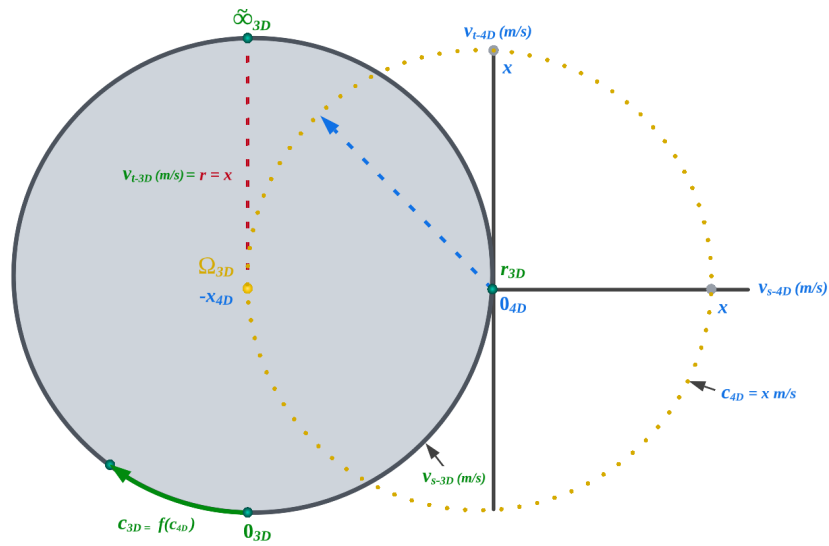


Fig. 6: A 4D+1 virtual photon to 3D+1 projection without scaling

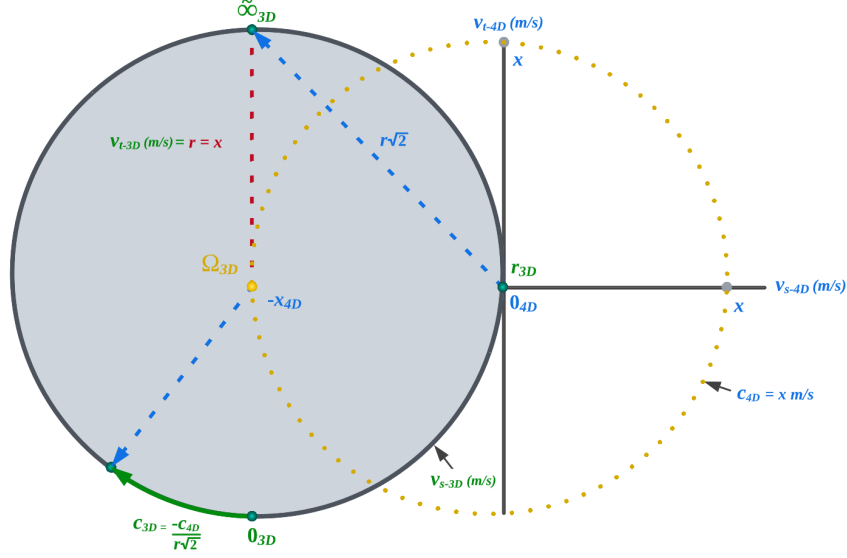


Fig. 7: 4D+1 to 3D+1 projective spacetime diagram

4.1 Plank units & Schwarzschild radius

I hypothesize that there is a significant correlation between the plank length [13] in this layer and the $4D+1$ black hole radius. In fact, they may even be identical. A theoretical validation of this hypothesis can be derived from configuring the Schwarzschild radius [2] equation to solve for the $4D+1$ speed of light as shown in Eq. (9). We can then insert plank units to solve for the $3D+1$ light-speed relationship. In Eq. (10) I demonstrate this plank-unit-Schwarzschild-radius property for the $4D+1$ and $3D+1$ light speeds. The resulting equation is similar, if not identical, to the projective spacetime diagram derivation if we infer the implicit l as the radius r of the higher-dimensional black hole from Eq. (8).

$$r_s = \frac{2GM}{c_4^2}$$

$$c_4^2 = \frac{2GM}{r_s} \quad (9)$$

$$c_4 = \sqrt{\frac{2GM}{r_s}}$$

$$\begin{aligned}
l_P = r_s &= \sqrt{\frac{\hbar G}{c^3}}, \quad m_P = M = \sqrt{\frac{\hbar c}{G}}, \quad c = c_3 \\
c_4 &= \sqrt{\frac{2GM}{r_s}} = \sqrt{\frac{2G\sqrt{\frac{\hbar c}{G}}}{\sqrt{\frac{\hbar G}{c^3}}}} \\
&= \sqrt{2G \frac{\sqrt{\hbar}\sqrt{c}}{\sqrt{G}} \cdot \frac{\sqrt{c^3}}{\sqrt{\hbar}\sqrt{G}}} = \sqrt{2G \frac{\sqrt{\hbar}\sqrt{c} c\sqrt{c}}{\sqrt{G}\sqrt{\hbar}\sqrt{G}}} \\
&= \sqrt{2G \frac{c^2}{G}} = \sqrt{2c^2} = c_3\sqrt{2} \\
c_3 &= \frac{c_4}{1 \cdot \sqrt{2}}
\end{aligned} \tag{10}$$

4.2 Validation of light projection scaling

If we do exist in a $4D+1$ black hole, and that black hole has an apparent horizon, then the black hole is evaporating energy through relativistic quantum effects theorized by Hawking radiation [31]. If that is the case, the $4D+1$ black hole is shrinking over time. If the exterior $4D+1$ radius is shrinking, then the projected speed of light on the $3D+1$ surface is, by definition, increasing.

The experiment I propose to test this hypothesis is derived from the work of Morton Spears [28]. The speed of light in a vacuum is related to permittivity, the interaction of a material by an external electric field, and permeability, the interaction of a material by an external magnetic field, through the relationship detailed in Eq. (11).

$$c = \frac{1}{\sqrt{\varepsilon_0\mu_0}} \tag{11}$$

Select either of the two properties to measure. I recommend measuring the vacuum permittivity, ε_0 , as dielectric capacitance may be simpler to implement and verify. Fix the other variables to their currently accepted constant values to take a snapshot in time. Pull a maximally sensitive vacuum and measure the vacuum permittivity for six months to a year. There should be a drop in permittivity at a rate of approximately one part per 13–15 billion (an almost imperceptible rate of change) in correlation to the period of a year and the approximate age of the universe. Note that the changing value of c may affect the anticipated ratio of the rate of change. Regardless, there should be a clear, statistically significant drop in the measured vacuum permittivity over time, which would then correlate to an increasing value of c as shown in Fig 8.

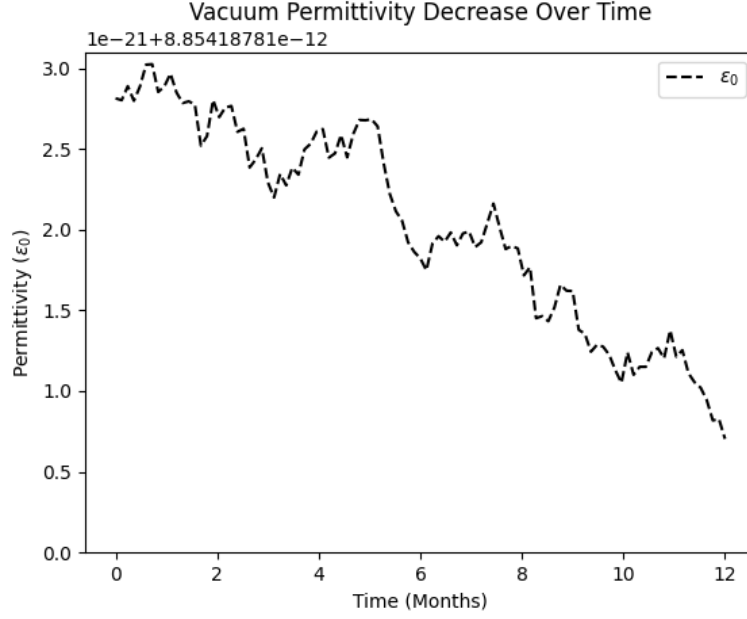


Fig. 8: Sample graph of ϵ_0 decreasing over a year

4.3 The camera obscura model

A projection passing through a plank-sized black hole can be modeled as a pinhole camera that maps a higher-dimensional object to a lower-dimensional image surface [32]. The diagram in Fig. 9 represents a homogeneous transform between an object in $4D$ camera Euclidean coordinates, $x/a, y/a, z/a, \& t/a, a = 1$, and a corresponding representation in $3D$ image Euclidean coordinates, $x/t, y/t, \& z/t$, through a singularity-sized pinhole. The focal length f is the spatial distance passed since the initial singularity point, the screen's pixel size is the plank length l_p , the projection size is the speed of light c , and the scaling factor is m_x . Eq. (12) defines the intrinsic camera matrix for this $4D$ to $3D$ cosmic camera.

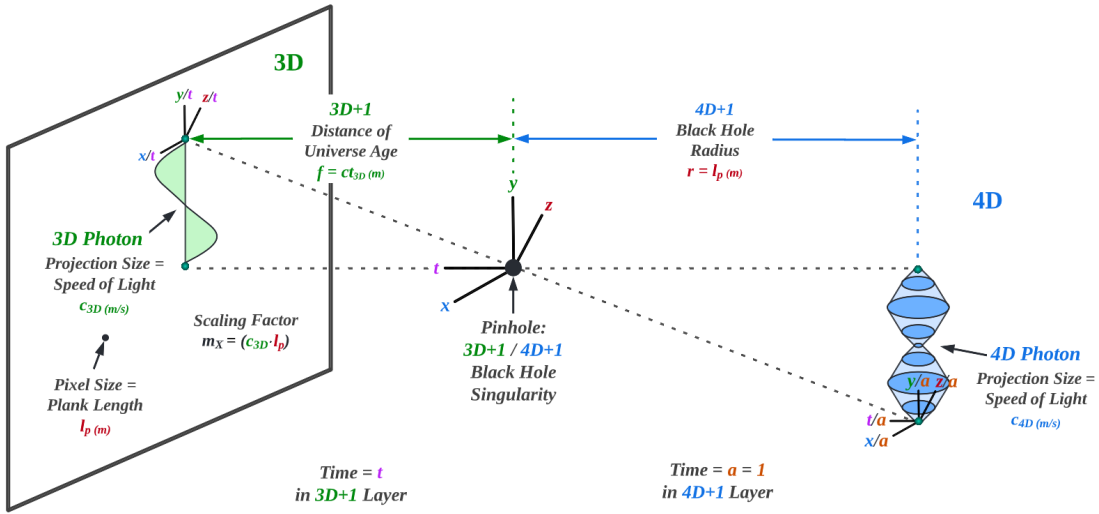


Fig. 9: The singularity pinhole camera model

$$\begin{aligned}
c_3 \begin{bmatrix} x/t \\ y/t \\ z/t \end{bmatrix} &= c_3 \begin{bmatrix} x \\ y \\ z \\ t \end{bmatrix} = \begin{bmatrix} f_x \cdot m_x & 0 & 0 & 0 & 0 \\ 0 & f_y \cdot m_y & 0 & 0 & 0 \\ 0 & 0 & f_z \cdot m_z & 0 & 0 \\ 0 & 0 & 0 & r_4 & 0 \end{bmatrix} \begin{bmatrix} x/a \\ y/a \\ z/a \\ t/a \\ 1 \end{bmatrix} c_4 \\
&= \begin{bmatrix} f_x(c_{3x} \cdot l_p) & 0 & 0 & 0 & 0 \\ 0 & f_y(c_{3y} \cdot l_p) & 0 & 0 & 0 \\ 0 & 0 & f_z(c_{3z} \cdot l_p) & 0 & 0 \\ 0 & 0 & 0 & l_p & 0 \end{bmatrix} \begin{bmatrix} x \\ y \\ z \\ t \\ a \end{bmatrix} c_4
\end{aligned} \tag{12}$$

Assuming that the given values for the plank length, the age of the universe in meters, and the speed of light are correct, the result of the intrinsic matrix formulation is relatively close to our previous geometric and Schwarzschild escape velocity calculations as shown in Eq. (13). To create the full multi-layered matrix equation for all ten dimensions, we have to take into account the intrinsic matrices from every layer. This is demonstrated at a high-level in Eq. (14).²

Although this is not explicitly derived in this paper, we also need to take into account the lens distortions that occur with time-scaled-spherical-light projections [11]. This may explain cosmological redshift [1] from a completely different perspective; however, finding evidence for this theoretically will require an adept team to create a complete cosmic-camera model.

$$\begin{aligned}
c_3 &= \frac{c_4}{1 \cdot \sqrt{2}} \\
&= 0.707 \cdot c_4 \\
c_3 &= f(c_3 \cdot l_p)c_4 \\
f &= 13.7 \cdot 10^9 y \\
&= 4.3 \cdot 10^{17} s (3 \cdot 10^8 m/s) \\
&= 1.3 \cdot 10^{26} m \\
c_3 &= 1.3 \cdot 10^{26} m (3 \cdot 10^8 m/s \cdot 1.6 \cdot 10^{-35} m)c_4 \\
c_3 &= 0.624 m^3/s \cdot c_4
\end{aligned} \tag{13}$$

$$c_3 \begin{bmatrix} x \\ y \\ z \\ t \end{bmatrix} = \begin{bmatrix} 4 X 5 \end{bmatrix} \begin{bmatrix} 5 X 6 \end{bmatrix} \begin{bmatrix} 6 X 7 \end{bmatrix} \begin{bmatrix} 7 X 8 \end{bmatrix} \begin{bmatrix} 8 X 9 \end{bmatrix} \begin{bmatrix} 9 X 10 \end{bmatrix} \begin{bmatrix} x \\ y \\ z \\ t \\ a \\ b \\ c \\ d \\ e \end{bmatrix} c_9 \tag{14}$$

²I do not see the use for computing the extrinsic matrices, as it is hard to imagine how translation and rotation can be determined in an external layer for a photon.

4.4 2D black holes & empty space

In this projection framework, black holes from collapsed stars that we observe are $2D+1$ lower-dimensional spaces. Objects cannot fall into a black hole; they flatten on the surface and lose a spatial dimension. For a $2D+1$ black hole, the new time projection is the previous layer's spatial dimension z . A new "fundamental force" is gained in a $2D+1$ black hole: the previous $3D+1$ layer's time component, t . This is shown in Fig. 10.

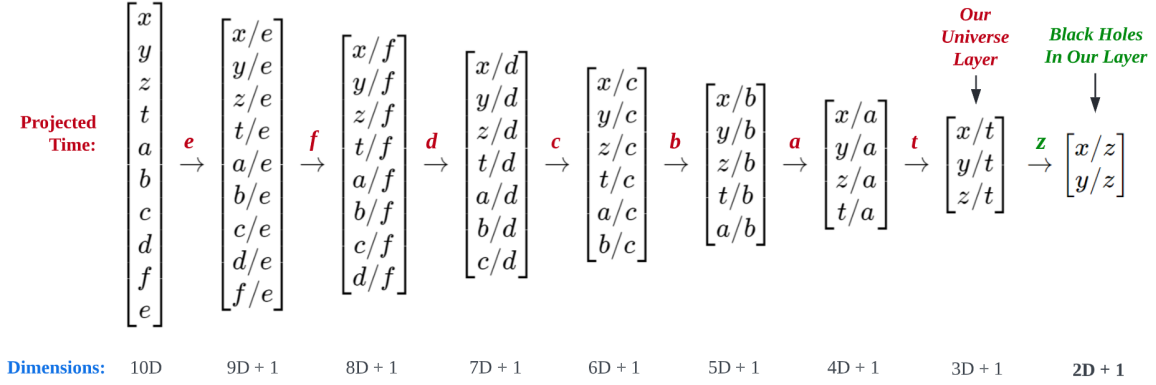


Fig. 10: 2D+1 black holes in our 3D+1 layer

This projection framework precludes the notion of "empty space" or a "true vacuum" in this $3D+1$ layer. Geometrically, it does not seem possible to enclose a $3D$ shape within a $4D$ space. If the known universe is the exterior surface of a $4D+1$ black hole and the $3D+1$ speed of light is a function of the higher-dimensional black hole radius and light speed, then there must be a minimum energy level required to maintain those parameters. This minimum energy level will appear as quantum fluctuations in the vacuum of $3D+1$ space. The visualization of the geometric argument is made in Fig. 11.

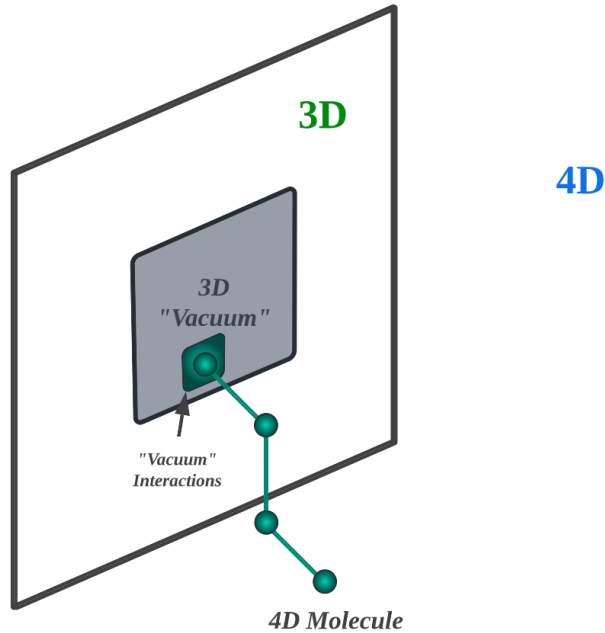


Fig. 11: The preclusion of "empty space"

5 The energy network

A connection between energy and artificial neural networks can be found in the stochastic version of a Hopfield network [27], also known as a Boltzmann machine [15]. This Boltzmann machine can be layered into a deep or multi-layered structure, which can then be applied to the projection framework as shown in Fig. 12.³ The physical implications from this energy model are as follows:

1. Time is a four-dimensional hidden layer that is formed from the combined interactions of six higher-dimensional hidden layers, $E, F, D, C, B, & A$.
2. The effects of the hidden layers $E, F, D, C, B, & A$ are perceived in the 3D output layer S , space, through the compression of the 4D hidden layer T , time.
3. 52 nodes and 322 separate connections with arbitrary weights exist.

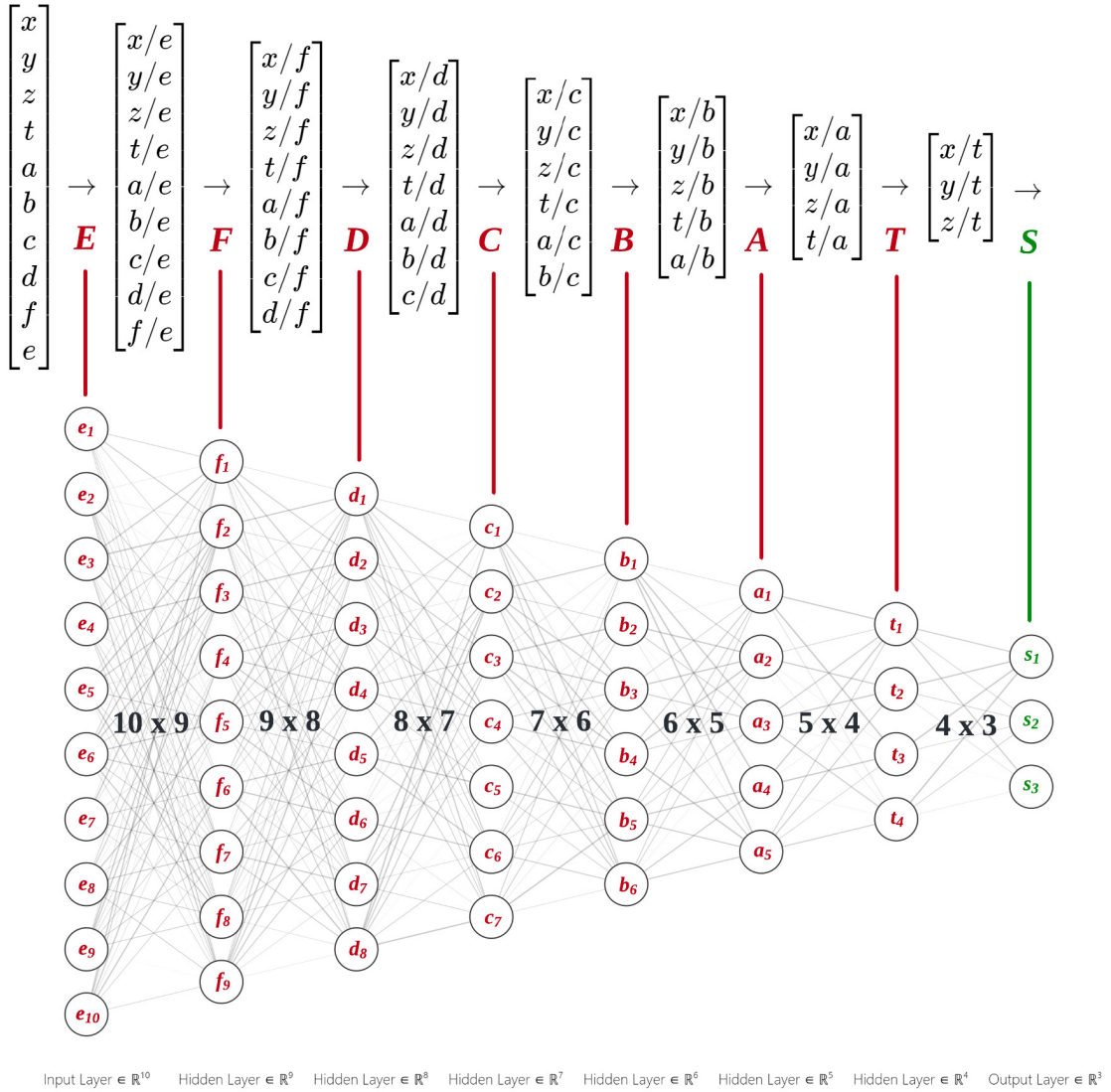


Fig. 12: The interconnected model of energy

³Note that Fig. 12 is in terms of a feedforward network to demonstrate the high-level structure.

Restricted Boltzmann machines (RBM) can be extended with complex number values as inputs and stacked to create deep artificial neural networks that characterize quantum many-body wave functions [5]. This structure has been used to describe the chiral boson CFT correlator wave function with 99.9% accuracy up to 22 visible spins, as described by Huan He et al. [14]. A single point in our observable layer can interact in the 3x4 RBM (space x time) but is influenced by the greater DRBM framework. The entire multi-layered structure operates by minimizing the free energy within every RBM as a collective, with the visible output of one layer becoming the hidden input of the next layer as shown in Fig. 13. The generalized equation to describe this layout is found in the same paper by Huan He et al. as shown in Eq. (15) [14]. This equation can be modified to fit the structure of our *10D-3D* multi-layered reality.

$$f_{k-RBM}(s_1, s_2, \dots, s_N) = \sum_{h_1^1, \dots, h_{m_1}^1} \sum_{h_1^2, \dots, h_{m_2}^2} \dots \sum_{h_1^k, \dots, h_{m_k}^k} \exp \left(\sum_{p_0, p_1} W_{p_0 p_1}^1 s_{p_0} h_{p_1}^1 \right) + \sum_{p_0} s_{p_0} a_{p_0} + \sum_{i=2}^k \sum_{p_{i-1}, p_i} W_{p_{i-1}, p_i}^i h_{p_{i-1}}^{i-1} h_{p_i}^i + \sum_{i=1}^k \sum_{p_i} h_{p_i}^i b_{p_i}^i \quad (15)$$

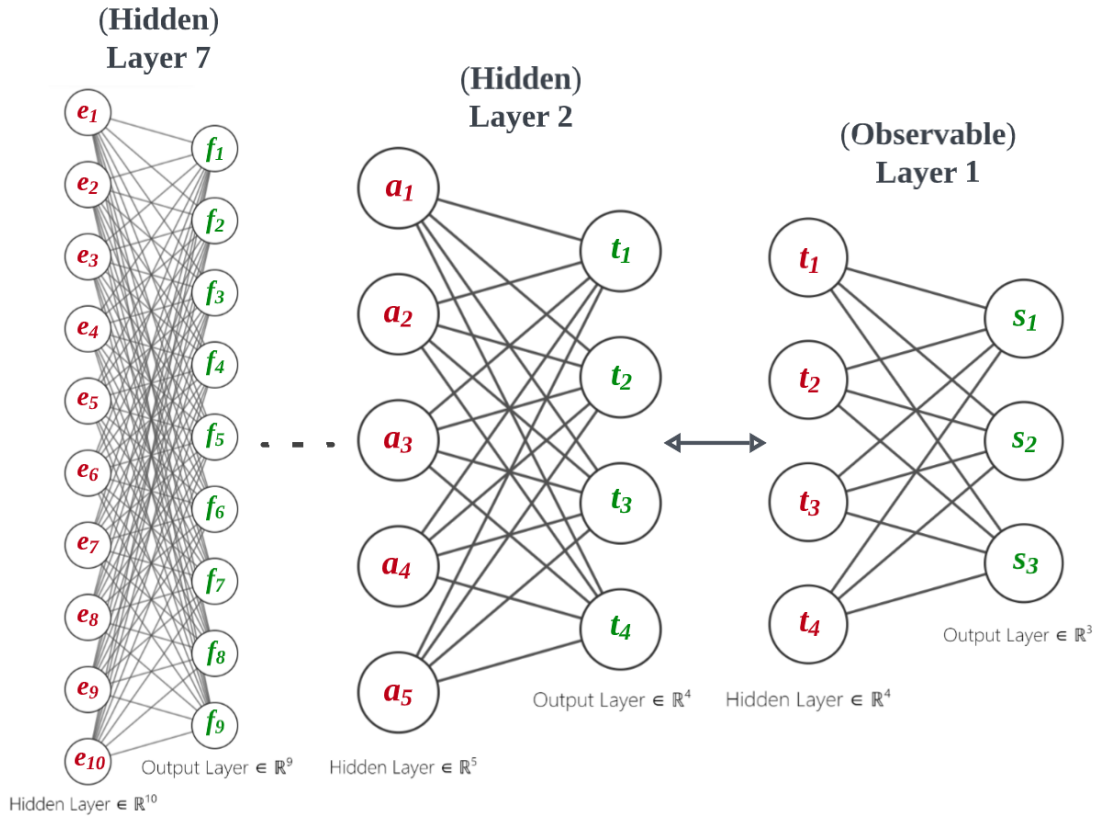


Fig. 13: The DRBM universe energy network

6 Conclusions

Quite a few simplifications and assumptions were made in this paper to gain intuition of the underlying physical structures. These simplifications must be addressed if an interconnected framework such as this is to become mathematically rigorous and accurately reflect reality. The vision of this paper is to formulate a systematic conceptual foundation for others to utilize, expand, and modify. While not employed in this paper, conformal geometric algebra [8] seems to be an appropriate language to precisely describe the mathematical structures of the overarching projective system.

7 Acknowledgements

I thank my wife, Lama, for proofreading this paper and ensuring that my equations and derivations were mathematically sound. I also thank Professor Donald D. Hoffman for taking the time to correspond to my emails about consciousness, perspective-dependent reality, and sending relevant papers related to these topics. His philosophical views of reality were foundational in inspiring me to think past spacetime to a more fundamental structure.

References

- [1] Elcio Abdalla et al. “Cosmology Intertwined: A Review of the Particle Physics, Astrophysics, and Cosmology Associated with the Cosmological Tensions and Anomalies”. In: (2022). DOI: 10.48550/ARXIV.2203.06142. URL: <https://arxiv.org/abs/2203.06142>.
- [2] Kazunori Akiyama et al. “First M87 Event Horizon Telescope Results. I. The Shadow of the Supermassive Black Hole”. In: *Astrophys. J. Lett.* 875 (2019), p. L1. DOI: 10.3847/2041-8213/ab0ec7. arXiv: 1906.11238 [astro-ph.GA].
- [3] Jose B. Almeida. *An hypersphere model of the Universe - The dismissal of dark matter*. 2004. DOI: 10.48550/ARXIV.PHYSICS/0402075. URL: <https://arxiv.org/abs/physics/0402075>.
- [4] Martin Bojowald. “Quantum cosmology: a review”. In: *Reports on Progress in Physics* 78.2 (Jan. 2015), p. 023901. DOI: 10.1088/0034-4885/78/2/023901. URL: <https://doi.org/10.1088%2F0034-4885%2F78%2F2%2F023901>.
- [5] Giuseppe Carleo and Matthias Troyer. “Solving the quantum many-body problem with artificial neural networks”. In: *Science* 355.6325 (Feb. 2017), pp. 602–606. DOI: 10.1126/science.aag2302. URL: <https://doi.org/10.1126%2Fscience.aag2302>.
- [6] Jesper Carlström. “Wheels – on division by zero”. In: *Mathematical Structures in Computer Science* 14.1 (2004), pp. 143–184. DOI: 10.1017/S0960129503004110.
- [7] Thibault Damour. *Poincare, Relativity, Billiards and Symmetry*. 2005. DOI: 10.48550/ARXIV.HEP-TH/0501168. URL: <https://arxiv.org/abs/hep-th/0501168>.
- [8] Chris Doran. *Circle and sphere blending with conformal geometric algebra*. 2003. arXiv: cs/0310017 [cs.CG].
- [9] A. Einstein. “Ist die Trägheit eines Körpers von seinem Energieinhalt abhängig?” In: *Annalen der Physik* 323.13 (1905), pp. 639–641. DOI: <https://doi.org/10.1002/andp.19053231314>. eprint: <https://onlinelibrary.wiley.com/doi/pdf/10.1002/andp.19053231314>. URL: <https://onlinelibrary.wiley.com/doi/abs/10.1002/andp.19053231314>.
- [10] A. Einstein. “Zur Elektrodynamik bewegter Körper”. In: *Annalen der Physik* 322.10 (1905), pp. 891–921. DOI: <https://doi.org/10.1002/andp.19053221004>. eprint: <https://onlinelibrary.wiley.com/doi/pdf/10.1002/andp.19053221004>. URL: <https://onlinelibrary.wiley.com/doi/abs/10.1002/andp.19053221004>.
- [11] Jinlong Fan et al. *Wide-angle Image Rectification: A Survey*. 2020. DOI: 10.48550/ARXIV.2011.12108. URL: <https://arxiv.org/abs/2011.12108>.
- [12] Chris Fields et al. “Eigenforms, interfaces and holographic encoding: Toward an evolutionary account of objects and spacetime”. In: *Constructivist Foundations* 12 (July 2017), pp. 265–274.
- [13] Luis J. Garay. “Quantum Gravity and Minimum Length”. In: *International Journal of Modern Physics A* 10.02 (Jan. 1995), pp. 145–165. DOI: 10.1142/s0217751x95000085. URL: <https://doi.org/10.1142%2Fs0217751x95000085>.
- [14] Huan He et al. *Multi-Layer Restricted Boltzmann Machine Representation of 1D Quantum Many-Body Wave Functions*. 2019. arXiv: 1910.13454 [cond-mat.str-el].
- [15] G. E. Hinton. “Boltzmann machine”. In: *Scholarpedia* 2.5 (2007), revision #91076, p. 1668. DOI: 10.4249/scholarpedia.1668.
- [16] Hengyuan Hu, Lisheng Gao, and Quanbin Ma. *Deep Restricted Boltzmann Networks*. 2016. DOI: 10.48550/ARXIV.1611.07917. URL: <https://arxiv.org/abs/1611.07917>.
- [17] Thomas Hurd. “The Projective Geometry of Simple Cosmological Models”. In: *Proceedings of The Royal Society A: Mathematical, Physical and Engineering Sciences* 397 (Feb. 1985), pp. 233–243. DOI: 10.1098/rspa.1985.0013.
- [18] Shau-Yu Lan et al. “A Clock Directly Linking Time to a Particle’s Mass”. In: *Science* 339.6119 (2013), pp. 554–557. DOI: 10.1126/science.1230767. eprint: <https://www.science.org/doi/pdf/10.1126/science.1230767>. URL: <https://www.science.org/doi/abs/10.1126/science.1230767>.

- [19] Sreenath K. Manikandan and Andrew N. Jordan. “Black holes as Andreev reflecting mirrors”. In: *Physical Review D* 102.6 (Sept. 2020). DOI: 10.1103/physrevd.102.064028. URL: <https://doi.org/10.1103/2Fphysrevd.102.064028>.
- [20] Saba Miyan and Jun Sato. “Reconstructing Sequential Patterns without Knowing Image Correspondences”. In: vol. E98.D. Nov. 2012, pp. 484–496. ISBN: 978-3-642-37446-3. DOI: 10.1007/978-3-642-37447-0_37.
- [21] J. Polchinski. *String theory. Vol. 2: Superstring theory and beyond*. Cambridge Monographs on Mathematical Physics. Cambridge University Press, Dec. 2007. DOI: 10.1017/CB09780511618123.
- [22] Razieh Pourhasan, Niayesh Afshordi, and Robert B. Mann. “Out of the white hole: a holographic origin for the Big Bang”. In: *Journal of Cosmology and Astroparticle Physics* 2014.04 (Apr. 2014), pp. 005–005. DOI: 10.1088/1475-7516/2014/04/005. URL: <https://doi.org/10.1088/2F1475-7516/2F2014/2F04/2F005>.
- [23] “Preface to the Second Edition”. In: *Quantum Information Theory*. Cambridge University Press, Nov. 2016, pp. xi–xii. DOI: 10.1017/9781316809976.001. URL: <https://doi.org/10.1017/2F9781316809976.001>.
- [24] Carlo Rovelli and Francesca Vidotto. *Covariant Loop Quantum Gravity: An Elementary Introduction to Quantum Gravity and Spinfoam Theory*. Cambridge University Press, 2014. DOI: 10.1017/CB09781107706910.
- [25] André Saraiva et al. “Photonic Counterparts of Cooper Pairs”. In: *Physical Review Letters* 119.19 (Nov. 2017). DOI: 10.1103/physrevlett.119.193603. URL: <https://doi.org/10.1103/2Fphysrevlett.119.193603>.
- [26] John H. Schwarz. “Status of Superstring and M-Theory”. In: *International Journal of Modern Physics A* 25.25 (Oct. 2010), pp. 4703–4725. DOI: 10.1142/s0217751x1005072x. URL: <https://doi.org/10.1142/2Fs0217751x1005072x>.
- [27] David Sherrington and Scott Kirkpatrick. “Solvable Model of a Spin-Glass”. In: *Phys. Rev. Lett.* 35 (26 Dec. 1975), pp. 1792–1796. DOI: 10.1103/PhysRevLett.35.1792. URL: <https://link.aps.org/doi/10.1103/PhysRevLett.35.1792>.
- [28] Morton Spears. “Permittivity Creates Dark Matter and an Older Universe with Accelerating Expansion”. In: *econ.iastate.edu* (July 1998). URL: <https://vixra.org/abs/2209.0168>.
- [29] Leonard Susskind. “The world as a hologram”. In: *Journal of Mathematical Physics* 36.11 (Nov. 1995), pp. 6377–6396. DOI: 10.1063/1.531249. URL: <https://doi.org/10.1063/2F1.531249>.
- [30] Wai-Shun Tong, Chi-Keung Tang, and Gérard Medioni. “Simultaneous two-view epipolar geometry estimation and motion segmentation by 4D tensor voting”. In: *IEEE transactions on pattern analysis and machine intelligence* 26 (Oct. 2004), pp. 1167–84. DOI: 10.1109/TPAMI.2004.72.
- [31] Matt Visser. “Essential and Inessential Features of Hawking Radiation”. In: *International Journal of Modern Physics D* 12.04 (Apr. 2003), pp. 649–661. DOI: 10.1142/s0218271803003190. URL: <https://doi.org/10.1142/2Fs0218271803003190>.
- [32] Zhengyou Zhang. “A Flexible New Technique for Camera Calibration”. In: *IEEE Transactions on Pattern Analysis and Machine Intelligence* 22 (Dec. 2000). MSR-TR-98-71, Updated March 25, 1999, pp. 1330–1334. URL: <https://www.microsoft.com/en-us/research/publication/a-flexible-new-technique-for-camera-calibration/>.